



HAL
open science

Impact of chronic doxycycline treatment in the APP/PS1 mouse model of Alzheimer's disease

Victoria Gomez-Murcia, Kevin Carvalho, Bryan Thiroux, Raphaëlle Caillierez, Melanie Besegher, Nicolas Sergeant, Luc Buée, Emile Faivre, David Blum

► To cite this version:

Victoria Gomez-Murcia, Kevin Carvalho, Bryan Thiroux, Raphaëlle Caillierez, Melanie Besegher, et al.. Impact of chronic doxycycline treatment in the APP/PS1 mouse model of Alzheimer's disease. *Neuropharmacology*, 2022, 209, pp.108999. 10.1016/j.neuropharm.2022.108999 . inserm-03699325

HAL Id: inserm-03699325

<https://inserm.hal.science/inserm-03699325>

Submitted on 22 Jul 2024

HAL is a multi-disciplinary open access archive for the deposit and dissemination of scientific research documents, whether they are published or not. The documents may come from teaching and research institutions in France or abroad, or from public or private research centers.

L'archive ouverte pluridisciplinaire **HAL**, est destinée au dépôt et à la diffusion de documents scientifiques de niveau recherche, publiés ou non, émanant des établissements d'enseignement et de recherche français ou étrangers, des laboratoires publics ou privés.



Distributed under a Creative Commons Attribution - NonCommercial 4.0 International License

1 **Impact of chronic doxycycline treatment in the APP/PS1 mouse model**
2 **of Alzheimer's Disease**

3
4 Victoria Gomez-Murcia^{1,2}, Kevin Carvalho^{1,2}, Bryan Thiroux^{1,2}, Raphaëlle Caillierez^{1,2},
5 Melanie Besegher³, Nicolas Sergeant^{1,2}, Luc Buée^{1,2}, Emile Faivre^{*1,2}, David Blum^{*1,2}

6
7 1. Univ. Lille, Inserm, CHU Lille, U1172 LilNCog - Lille Neuroscience & Cognition,
8 Lille, France.
9 2. Alzheimer & Tauopathies, LabEx DISTALZ, France.
10 3. Univ. Lille, CNRS, Inserm, CHU Lille, Institut Pasteur de Lille, US 41 - UMS 2014 -
11 PLBS, Animal Facility, F-59000 Lille, France.

12

13

14 *Equal contribution

15

16

17

18

19 # Correspondence to: David Blum, Inserm UMR-S1172, “Alzheimer & Tauopathies”,
20 Place de Verdun, 59045, Lille Cedex, France. Orcid Number: 0000-0001-5691-431X.
21 Tel: +33320298850, Fax: +33320538562. david.blum@inserm.fr

22

23

24 **Conflict of interest.** The authors have declared that they have no conflict of interest.

25

26 **ABSTRACT**

27

28 Due to the pathophysiological complexity of Alzheimer's disease, multitarget
29 approaches able to mitigate several pathogenic mechanisms are of interest. Previous
30 studies have pointed to the neuroprotective potential of Doxycycline (Dox), a safe and
31 inexpensive second-generation tetracycline. Dox has been particularly reported to slow
32 down aggregation of misfolded proteins but also to mitigate neuroinflammatory
33 processes. Here, we have evaluated the pre-clinical potential of Dox in the APP/PS1
34 mouse model of amyloidogenesis. Dox was provided to APP/PS1 mice from the age of
35 8 months, when animals already exhibit amyloid pathology and memory deficits.
36 Spatial memory was then evaluated from 9 to 10 months of age. Our data demonstrated
37 that Dox moderately improved the spatial memory of APP/PS1 mice without exerting
38 major effect on amyloid lesions. While Dox did not alleviate overall glial reactivity, we
39 could evidence that it rather enhanced the amyloid-dependent upregulation of several
40 neuroinflammatory markers such as CCL3 and CCL4. Finally, Dox exerted
41 differentially regulated the levels of synaptic proteins in the hippocampus and the cortex
42 of APP/PS1 mice. Overall, these observations support that chronic Dox delivery does
43 not provide major pathophysiological improvements in the APP/PS1 mouse model.

44

45

46 **KEYWORDS**

47 Doxycycline; Alzheimer's Disease; mouse model

48

49

50

51 INTRODUCTION

52

53 Alzheimer's disease (AD) is a neurodegenerative disorder defined by the presence of
54 two
55 neuropathological lesions: intraneuronal aggregates of hyperphosphorylated Tau
56 proteins and extracellular accumulation of toxic A β peptides, generated by the
57 sequential cleavages of the Amyloid Precursor Protein (APP; for a review see (Müller et
58 al., 2017). In addition, neuroinflammation - characterized by the pathological reactivity
59 of microglial and astrocytic cells as well as the release of various cytokines/chemokines
60 - develops along with AD brain lesions (Heneka et al., 2018; Laurent et al., 2018).
61 These pathological changes promote early synaptic dysfunctions, notably at forebrain
62 glutamatergic synapses (Canas et al., 2014; Dennis J. Selkoe, 2002; Kirvell et al., 2006)
63 and, subsequently, synapse loss leading to the progressive development of cognitive
64 deficits.

65 Due to the pathophysiological complexity of AD, multitarget approaches to mitigate at
66 the same time several pathological mechanisms (protein aggregation,
67 neuroinflammation, neuronal loss...) might be of interest. Previous studies have pointed
68 to the neuroprotective effects of tetracyclines, a class of antibiotics, against
69 neurodegenerative and neuroinflammatory conditions (D. Orsucci, V. Calsolaro, M.
70 Mancuso, 2009). Among tetracyclines, doxycycline (6-Deoxy-5-hydroxytetracycline;
71 Dox) is a safe and inexpensive second-generation tetracycline which has demonstrated
72 safe toxicological profile, even after long-lasting administration (Haïk et al., 2014) and
73 good brain penetration (Domercq and Matute, 2004). Dox has been reported to exhibit
74 neuroprotective properties in a large range of neurodegenerative models not only thanks
75 to its ability to slow down aggregation of misfolded proteins but also to mitigate

76 neuroinflammatory processes and enhance neurogenesis (for review see (Santa-Cecília
77 et al., 2019; Sultan et al., 2013). In particular, Dox inhibit A β 42 aggregation and
78 disassemble preformed fibrils (Forloni et al., 2001). Accordingly, in *Caenorhabditis*
79 *elegans* and drosophila models of A β toxicity, Dox was found to mitigate A β
80 proteotoxicity, by interacting with A β assemblies and reducing formation of amyloid
81 aggregates, thereby improving motor behavior (Costa et al., 2011; Diomedede et al.,
82 2010). Only one study evaluated the potential impact of Dox in an animal model of AD.
83 (Balducci et al., 2018) tested its efficacy in the APP/PS1 mouse model of
84 amyloidogenesis. This study showed that subchronic i.p. treatment (20 days or 2
85 months) with the antibiotic restored recognition memory in aged APP/PS1 animals
86 without impacting cortical A β plaques. This effect on memory was confirmed by the
87 same authors in another mouse model induced by i.c.v injection of A β oligomers. In
88 both models, the benefit observed was associated with a lower neuroinflammation.
89 In the present study, we extended this former work and evaluated the impact of chronic
90 Dox delivery in mid-aged APP/PS1 mice and found that while Dox exerted a significant
91 impact in alleviating spatial memory impairments in two spatial memory tasks, without
92 exerting major effect on amyloid lesions, we could evidence paradoxical effects towards
93 inflammatory and synaptic markers in the hippocampus and the cortex. These
94 observations support that the clinical use of Dox should be considered with caution in
95 the context of AD.

96

97 MATERIAL AND METHODS

98

99 **Animals.** Heterozygous male APP^{swe}/PS1^{dE9} mice (41 in total) were used in this
100 study (herein referred to as APP/PS1, C57Bl6/J background; (Jankowsky et al., 2001)

101 together with littermates controls (WT). All animals were maintained in standard cages
102 under conventional laboratory conditions (12 h/12 h light/dark cycle, 22°C), with ad
103 libitum access to food and water. Mice were maintained 5–6 per cage. The animals were
104 used in compliance with European standards for the care and use of laboratory animals
105 and experimental protocols approved by the local Animal Ethical Committee (CEEA75,
106 Lille, France).

107

108 **Treatment.** To avoid potential stress associated with multiple i.p. injections or gavage,
109 animals were orally treated through drinking water with Doxycycline hydrochloride
110 (Thermo Fisher; 0.4 mg/mL in 2.5% sucrose) or with 2.5% sucrose, in control
111 conditions. Animals were randomized into four experimental groups: WT-Sucrose
112 (WT), WT-Dox (WT Dox), APP/PS1-Sucrose (APP), APP/PS1-Dox (APP Dox).
113 Doxycycline solution was kept in dark bottles protected from light and changed 3 times
114 per week. Considering the average intake measured along the treatment and the body
115 weight of mice, the oral Dox treatment corresponded to circa. 50 mg/kg i.e. in the range
116 providing protection to APP/PS1 mice as shown in (Balducci et al., 2018). Treatment
117 started from 8 months of age - at a time amyloid pathology and memory deficits are
118 already present in this strain (Zhou et al., 2015) - i.e. one month before behavioral
119 experiments; and animals were kept under Vehicle or Dox until the end of the
120 experimental procedure i.e. 9-10 months of age.

121

122 **Behavioral studies.** All the animals underwent all the behavioral tests described below
123 in a blind manner. An interval of 48h was respected between each task.

124

125 **Actimetry.** Mice were placed in the center of an infrared Actimeter (45x45x35cm;
126 Bioseb), composed by a 2-dimensional square frame, and left for 10 min. Spontaneous
127 behavior of mice was tracked with distance travelled and velocity recorded by Actitrack
128 software (Bioseb).

129 **Y-maze task.** Short-term spatial memory was assessed in a spontaneous novelty-based
130 spatial preference Y-maze test. All arms of the Y-maze were 28 cm long, 6.2 cm wide,
131 with 15-cm-high white opaque walls. Different extra maze cues (elements of different
132 colors and shapes such as yellow plastic bag, a black rectangular box and a panel with
133 red and black circles) were placed on the surrounding walls. To avoid intra-maze odor
134 cues, sawdust was placed in the maze and mixed between each phase. Allocation of
135 arms was counterbalanced within each group. During the learning phase, mice were
136 placed at the end of the 'start' arm and were allowed to explore the 'start' arm and the
137 'other (familiar)' arm for 5 min (beginning from the time the mouse first left the start
138 arm). Access to the third arm of the maze ('novel' arm) was blocked by an opaque door.
139 The mouse was then removed from the maze and returned to its home cage for 2 min. In
140 the test phase the mouse was placed again in the 'start' arm of the maze, the door of the
141 'novel' arm was removed, and mouse behavior recorded for one minute (from the time
142 the mouse first left the start arm). The amount of time the mouse spent in each arm of
143 the maze was recorded during both learning and test phases using EthovisionXT
144 (Noldus Information Technology, Wageningen, The Netherlands). For the learning
145 phase, we calculated the percentage of time spent in the 'other' (familiar) arm vs. the
146 'start' arm. For the test phase, a discrimination index $[\text{novel arm}/(\text{novel}+\text{familiar arm})]$
147 $\times 100$ was calculated.

148

149 ***Barnes Maze Task.*** Spatial learning and memory were evaluated using the Barnes maze
150 task. This behavioral apparatus is a white circular PVC open platform surface (120 cm
151 of diameter) with 40 equally spaced holes (5 cm of diameter) located at 5 cm from its
152 circumference and a black escape box located under one of the 40 holes. The platform is
153 placed on a swivel system (to rotate it easily) in the center of the room, elevated 80 cm
154 above the floor, enlighten by a flood light (800 lux) placed above and surrounded by
155 spatial cues. Mice completed a habituation trial to become familiar with the circular
156 platform environment and to practice descending into the escape box. Mice were free
157 for 5 min to explore the area around the escape hole and the escape box. Then, mice
158 completed 4 days of acquisition training (learning phase) with 4 trials per day. For each
159 trial, mice were placed in the start tube in the center of the circular platform (for 5-10 s)
160 and then trained to locate the escape hole (randomized for all mice) using spatial cues
161 (panels with different colors and shapes place on the wall such as a pink heart, yellow
162 face and black and white stripes flag) surrounding the platform. If a mouse did not enter
163 into the escape hole in 3 min it was gently guided to the escape hole. Mice remained 60s
164 in the escape box before returned to its home cage. The inter-trial interval was 15 min.
165 To reduce possible odor cues, the platform surface and escape box were cleaned with
166 70% Ethanol between each trial and the circular platform was rotated clockwise a
167 quarter turn every day. For each trial, path length to enter the escape box was recorded
168 using the Ethovision XT tracking system (Noldus). 24h after the last day of the training,
169 mice completed a 90s probe trial where the escape box was removed. The time spent in
170 the Target quadrant (T) versus average non-target quadrants (O) was determined.

171

172 ***Sacrifice and Brain Tissue Preparation.*** To sacrifice animals, they were deeply
173 anesthetized with a mixture of ketamine/xylazine, then transcardially perfused with cold

174 NaCl (0.9%). The brain was then removed. One hemisphere was post-fixed in 4%
175 paraformaldehyde fixative in PBS (pH 7.4) for 24h at 4°C and transferred to 30%
176 sucrose solution before being frozen at -40°C in isopentane (methyl-butane). Brains
177 were cut in coronal floating sections (35 µm) using a Leica cryostat and stored in PBS-
178 azide (0.2%) at 4°C. For each animal, 6-7 sections were collected per animal from
179 bregma -1.46mm to bregma -3.08mm, encompassing the whole hippocampus. The other
180 hemisphere was used for biochemical assays and cortex and hippocampus were
181 dissected out 4°C and stored at -80°C.

182

183 **Biochemical analyses.** For all biochemical experiments, tissue was homogenized in 200
184 µL Tris buffer (pH 7.4) containing 10% sucrose, sonicated, and kept at -80°C until use.
185 Protein amounts were evaluated using the BCA assay (Pierce), subsequently diluted
186 with lithium dodecyl sulfate (LDS) 2X supplemented with reducing agents (Invitrogen)
187 and then separated on 4-12% Criterion Bis-Tris Gels (Invitrogen). For total A β (6E10),
188 A β 42 (21F12) and C-terminal fragments (CTFs), proteins were separated on 16.5%
189 Criterion Gel Tris tricine (Invitrogen). Proteins were transferred to nitrocellulose or
190 PVDF membranes, which were then saturated (5% non-fat dry milk or 5% BSA) in
191 TNT (Tris 15mM pH8, NaCl 140mM, 0.05% Tween) and respectively incubated with
192 primary (see **Table 1**) overnight and corresponding secondary antibodies: peroxidase
193 labeled horse anti-rabbit and anti-mouse (1/5000 and 1/50000 respectively, Vector
194 Laboratories). Signals were visualized using chemiluminescence kits (ECLTM,
195 Amersham Bioscience) and a LAS4000 imaging system (Fujifilm). Results were
196 normalized to β -actin or GAPDH and quantifications were performed using ImageJ
197 software.

198

199 **ELISA.** Brain levels of human A β 1-40 and A β 1-42 were measured using ELISA kits
200 (Invitrogen, CA, USA; IBL-International, Hamburg, Germany) following
201 manufacturer's instructions. For hippocampal and cortical samples, A β was first
202 extracted as described previously (Faivre et al., 2018). Briefly, 20 μ g of protein were
203 diluted in Guanidine/Tris buffer. Samples were then diluted in a Dulbecco's phosphate
204 buffered saline containing 5% BSA and 0.03% Tween-20 (BSAT-DPBS) solution. The
205 homogenates were centrifuged, and supernatants were collected for the analysis of A β 1-
206 40 and A β 1-42 by colorimetric immunoassays. To measure levels of human A β
207 oligomers we used the 82E1-specific ELISA kit (IBL-International, Hamburg,
208 Germany). 20 μ g of proteins in tris sucrose buffer were used for this analysis. In all
209 cases, absorbances were measured by Multiskan Ascent counter (ThermoLab Systems).
210 The normalized amounts of A β and A β oligomers were expressed as pg/mL or pmol/L,
211 respectively.

212

213 **Immunohistochemistry and Image Analysis.** All antibodies used in this study are
214 detailed in **Table 1**. For A β immunohistochemistry (IHC), sections were first pretreated
215 with 80% formic acid for 3 min, after washing them in water, they were permeabilized
216 with 0.2% Triton X-100/sodium phosphate buffer. Sections were then blocked with
217 10% "Mouse On Mouse" Kit serum (Vector Laboratories) for 1 h before incubation
218 with mouse biotinylated anti-A β antibody (6E10) at 4°C overnight. After washing in
219 PBS, labelling was amplified by the application of the avidin-biotin-HRP complex
220 (ABC kit, 1:400 in PBS, Vector) prior to addition of diaminobenzidine
221 tetrahydrochloride (DAB, Vector) in Tris-HCl 0.1 mol/l, pH 7.6, containing H₂O₂ for
222 visualization. Brain sections were then mounted, air-dried, dehydrated by passage
223 through a graded series of alcohol (70%, 95%, 100%) and toluene baths, and finally

224 mounted with VectaMount (Vector Laboratories). For Iba1 and GFAP
225 immunohistochemistries, sections were first permeabilized with 0.2% Triton X-
226 100/sodium phosphate buffer. Sections were then blocked with 1/100 normal goat
227 serum (Vector Laboratories) for 1 h before incubation with rabbit anti-GFAP and rabbit
228 anti-Iba1 antibody at 4°C overnight. After washing in PBS, the sections were incubated
229 with anti-rabbit secondary biotinylated antibody (Vector BA-1000) during 1h in 0.2%
230 Triton X-100/sodium phosphate buffer. After washing in PBS, the sections were
231 incubated with the ABC kit developed using DAB, mounted, and dehydrated as before.
232 For blinded quantification, section imaging was performed using a slide scanner
233 (Axioscan Z1-Zeiss) with a 20× objective. Brain sections were analyzed using Mercator
234 image analysis system (Explora Nova, La Rochelle, France) using hue, saturation, and
235 intensity to distinguish objects in the image field. Thresholds were established manually
236 using identified objects on a set of slides and these segmentation thresholds remained
237 constant throughout the analysis. ROIs were outlined as follows: for the hippocampus,
238 the whole hippocampal signal was measured in each animal all along the rostral-caudal
239 axis and averaged; for the cortex, the signal was measured all along the rostral-caudal
240 axis from the dorsal part of visible cortex (retrosplenial cortex) to the more ventral part
241 of the cortex (excluding the piriform). Results are presented either as per cent marker
242 occupancy (immunoreactive area normalized to the whole area analyzed) or the number
243 of plaques and the average plaque size expressed as percentage of analyzed area.

244

245 ***RNA extraction and quantitative real-time PCR analysis (RT-qPCR).*** Total RNA was
246 extracted from hippocampi and cortex and purified using the RNeasy Lipid Tissue Mini
247 Kit (Qiagen, France). 500 nanograms of total RNA was reverse-transcribed using the
248 Applied Biosystems High-Capacity cDNA reverse transcription kit. Quantitative real-

249 time RT-PCR analysis was performed on an Applied Biosystems Prism 7900 System
250 using Power SYBR Green PCR Master Mix. The thermal cycler conditions were as
251 follows: hold for 10 min at 95°C, followed by 45 cycles of a two-step PCR consisting of
252 a 95°C step for 15 s followed by a 60°C step for 25 s. Sequences of primer used are
253 given in **Table 2**. Cyclophilin A was used as a reference housekeeping gene for
254 normalization. Amplifications were carried out in triplicate and the relative expression
255 of target genes was determined by the $\Delta\Delta\text{CT}$ method.

256

257 **Statistics.** Results were expressed as means \pm SEM. Differences between groups were
258 determined using unpaired Student's t-test, One-sample t-test or Two Way-analysis of
259 variance (ANOVA) followed by a Tukey's post-hoc multiple comparison test using
260 GraphPad Prism Software. P values < 0.05 were considered significant.

261

262 **RESULTS**

263

264 **Chronic doxycycline prevents spatial memory in APP/PS1 mice.** Eight month-old
265 WT and APP/PS1 mice were orally treated with Dox through drinking water (0.4
266 mg/mL circa 50 mg/kg), 4 weeks before behavioral evaluations, at a time APP/PS1
267 mice have been shown exhibit amyloid pathology and memory deficits (Zhou et al.,
268 2015).

269 We first evaluated spontaneous locomotion using actimetry (**Figures 1A**) and found no
270 significant effect of genotype ($F(1,32)=1.82$; $P=0.18$; Two-way ANOVA) and Dox
271 treatment ($F(1,32)=0.26$, $P=0.61$); Similarly, distance travelled (**Figures 1B**) was not
272 affected (Genotype: $F(1,32)=1.88$, $P=0.18$; Treatment: $F(1,32)=0.31$, $P=0.58$; Two-way
273 ANOVA).

274 Then, we determined the impact of the treatment on both short and long-term spatial
275 memory, using Y-maze and Barnes-maze tasks, respectively. In the Y-maze task, during
276 the learning phase, all groups explored the maze equally, spending a similar amount of
277 time in the two available arms (Genotype: $F(1,33)=0.56$, $P=0.45$; Treatment:
278 $F(1,33)=0.72$, $P=0.40$; Two-way ANOVA; **Figure 1C**). During the test phase, using
279 Two-Way ANOVA, we could not evidence any difference in the discrimination index
280 regarding genotype ($F(1,33)=0.51$, $P=0.48$), treatment ($F(1,33)=2.34$, $P=0.13$) or their
281 interaction ($F(1,33)=1.58$, $P=0.21$; **Figure 1C**). It was however notable that the
282 discrimination index was significantly above chance (i.e. 50%; **Figure 1C, dashed line**)
283 for WT ($P=0.05$; One sample t-test), WT Dox ($P<0.001$) and APP Dox ($P<0.001$) but
284 not APP ($P=0.43$), suggesting that Dox might improve short-term memory in APP/PS1
285 mice.

286 Next, we evaluated long-term spatial memory using the Barnes maze. During the
287 learning phase, all groups showed a decrease in path length across trials (Time: F
288 $(3,108)=59.66$, $P<0.0001$) in a similar manner between groups with no difference
289 among genotypes ($F(1,37)=0.88$, $P=0.35$) nor genotype x treatment x time interaction
290 ($F(3,108)=1.81$, $P=0.14$; RM Two-way ANOVA; **Figure 1E**), indicative of a proper
291 spatial learning abilities in all groups. 24 hours following acquisition, a probe trial was
292 performed to assess spatial memory. The time spent in the target quadrant was found
293 different between genotypes ($F(1,36)=6.86$, $P=0.01$), with a significant difference
294 observed between WT and APP mice ($P<0.01$; Two-way ANOVA followed by Tukey's
295 post-hoc test), indicating memory impairment of APP/PS1 mice. While the post-hoc
296 analysis could not show a significant difference between APP and APP dox animals
297 ($P=0.17$), a significant genotype x treatment interaction could be observed
298 ($F(1,36)=6.05$; $P=0.02$) and the percentage of time spent in the target quadrant by APP

299 Dox mice was found similar to WT ($P=0.55$, Two-Way ANOVA followed by Tukey's
300 post-hoc analysis). In the Barnes Maze, proper memory is acknowledged by a
301 percentage of time spent in the target quadrant significantly above 25%. Interestingly,
302 while APP mice did not reach that cut-off ($P=0.46$; One-Sample t-test, **Figure 1F**,
303 **dashed lines**), WT ($P<0.0001$), WT Dox ($P<0.01$) but also APP Dox ($P<0.01$) animals
304 exhibited a percentage of time spent in the target quadrant largely above chance,
305 supporting a beneficial influence of Dox towards memory of APP/PS1 animals.
306 Altogether, behavioral assessments support a moderate but beneficial impact of Dox to
307 the memory deficits of APP/PS1 mice.

308

309 **Impact of Doxycycline on amyloid pathology in the hippocampus and the cortex of**
310 **APP/PS1 transgenic mice.** Age-dependent spatial memory impairment in APP/PS1 has
311 been shown to correlate with increased brain amyloid burden (Garcia-Alloza et al.,
312 2006; Savonenko et al., 2005; Zhang et al., 2012). We therefore evaluated the potential
313 impact of Dox treatment on amyloid load and APP metabolism in APP/PS1 mice. First,
314 the concentrations of A β 1-42 and A β 1-40 were found similar in the hippocampus of
315 APP/PS1 mice treated with vehicle or Dox (A β 1-42: $P=0.37$; A β 1-40: $P=0.44$; A β 1-42/
316 A β 1-40: $P=0.87$ in APP/PS1 Dox vs. Vehicle; Student's t-test; **Figure 2A**). Also, we
317 could not observe difference between these groups in both the cortex (A β 1-42: $P=0.65$;
318 A β 1-40: $P=0.65$; A β 1-42/ A β 1-40: $P=0.61$) and the plasma (A β 1-42: $P=0.96$; A β 1-40:
319 $P=0.37$; A β 1-42/ A β 1-40: $P=0.11$). We also quantified A β oligomers in the
320 hippocampus and the cortex of both APP/PS1 groups (**Figure 2B**). Although no change
321 was observed in the hippocampus ($P=0.72$ in APP/PS1 Dox vs. Vehicle; Student's t-
322 test; **Figure 2B**), A β oligomers were found significantly enhanced in the cortex of
323 APP/PS1 treated with Dox ($P<0.001$ in APP/PS1 Dox vs. Vehicle; Student's t-test;

324 **Figure 2B**). In addition, we analyzed hippocampal and cortical amyloid plaques using
325 6E10 immunohistochemistry (**Figures 2C**). The area covered by plaques in the
326 hippocampus and the cortex remained similar between APP and APP Dox animals
327 (Hippocampus: $P=0.99$; Cortex: $P=0.21$, APP/PS1 Dox vs. Vehicle using Student's t-
328 test; **Figures 2D**). In the hippocampus, chronic treatment with Dox did not significantly
329 alter the density of amyloid plaques of low (50-250 μ m) or large (250-500 μ m) size
330 (**Figure 2D**; Hippocampus: $F(1,14)=0.005$, $P=0.93$, Cortex: $F(1,14)=2.13$, $P=0.16$ vs.
331 APP/PS1 using RM Two-Way ANOVA). Finally, we evaluated the APP metabolism in
332 both APP/PS1 groups. In the hippocampus, no difference could be observed between
333 APP/PS1 vehicle and Dox regarding levels of APP, APP carboxy-terminal fragments
334 (CTFs), total A β (6E10) or A β_{42} (21F12) levels) (**Figure 2E**). In the cortex, APP level
335 was slightly increased in the Dox group ($P= 0.02$, in APP/PS1 Dox vs. Vehicle;
336 Student's t-test; **Figure 2F**) while CTFs, total A β and A β_{42} were not modified (**Figure**
337 **2F**). These data indicated that, overall, Dox is ineffective to alter amyloidogenesis in
338 both cortex and hippocampus of APP/PS1 mice.

339

340 **Effect of chronic Doxycycline treatment on neuroinflammatory markers in the**
341 **hippocampus and the cortex of APP/PS1 mice.** Amyloid pathology is known to
342 promote microglial and astrocytic reactivity and a chronic pro-inflammatory
343 environment, favoring the development of memory deficits (Heneka et al., 2018).
344 Moreover, Dox was previously demonstrated to exhibit anti-neuroinflammatory
345 properties, particularly in an amyloid context (Balducci et al., 2018). Therefore, we first
346 evaluated the outcome of Doxycycline treatment towards glial cell activation through
347 IHC immunoreactivity for Iba1 (microglia) and GFAP (astrocytes), in the hippocampus
348 and the cortex of WT and APP/SP1 mice treated with vehicle and Dox (**Figure 3A-B**).

349 While 9m-old APP/PS1 mice exhibit reactivity of microglia (Cortex: $F(1,23)=30.60$,
350 $P<0.001$; Hippocampus: $F(1,22)=29.74$, $P<0.001$; **Figure 3A**) and astrocytes (Cortex:
351 $F(1,22)=25.01$, $P<0.001$ vs. WT; **Figure 3B**) as compared to WT animals, Dox modified
352 none of these glial activations. In addition, we also evaluated glial and
353 neuroinflammatory markers in the hippocampus and the cortex of all mouse groups
354 using qPCR. Overall, data clearly showed the upregulation of most of the glial and
355 neuroinflammatory markers studied in both the hippocampus and the cortex of APP/PS1
356 mice as compared to WT animals (**Figures 4A-B**). In the hippocampus (**Figure 4A**),
357 while most markers (GFAP, CD68, TLR2 C1qa, TNF α) were not significantly modified
358 by the Dox treatment in APP/PS1 mice, several of them were surprisingly found
359 upregulated by the tetracycline such as CCL3 ($F(1,35)=9.70$, $P=0.004$; $P<0.01$, APP vs.
360 APP Dox using Two-way ANOVA followed by Tukey's post-hoc test), CCL4
361 ($F(1,36)=10.34$; $P=0.003$; $P<0.01$, APP vs. APP Dox), Clec7a ($F(1,35)=14.46$,
362 $P<0.001$; $P<0.001$, APP vs. APP Dox) and Itgax ($F(1,33)=24.30$, $P<0.001$; $P<0.0001$,
363 APP vs. APP Dox). In the cortex (**Figure 4B**), most of the glial and inflammatory
364 makers were also upregulated in APP/PS1 mice as compared to WT animals but were
365 not significantly altered by Dox, with the exception of CCL4, upregulated as compared
366 with APP/PS1 animals ($F(1,28)=6.369$, $P=0.02$; $P<0.01$, APP vs. APP Dox). Overall,
367 our data suggest that Dox potentiate the amyloid-induced upregulation of neuro-
368 inflammatory markers in APP/PS1 mice, with a most effective impact at the
369 hippocampal level.

370

371 **Effect of chronic Doxycycline treatment on hippocampal and cortical synaptic**
372 **markers in APP/PS1 mice.** Finally, we evaluated, in APP/PS1 mice, the impact of Dox
373 treatment on the level of various synaptic markers (AMPA and NMDA receptors,

374 pre/post-synaptic markers). In the hippocampus, we did not observe change in the
375 amount of NMDA receptor subunits (NR1, NR2A, NR2B) as well as for GluR2 and
376 PSD95. Interestingly, GluR1 was found increased in the hippocampus of APP/PS1 after
377 Dox treatment ($+27.6 \pm 4.5\%$ vs APP/PS1, $P < 0.001$ using Student's *t*-test; **Figure 5A**).
378 Dox treatment also enhanced the level of the pre-synaptic SNAP25 protein
379 ($+46.2 \pm 17.1\%$ vs APP/PS1, $P = 0.05$ using Student's *t*-test; **Figure 5A**) as well as the
380 post-synaptic Cofilin protein ($+114.7 \pm 2.6\%$ vs APP/PS1, $P < 0.001$ using Student's *t*-
381 test; **Figure 5A**). However, Munc18 was found downregulated in mice treated with Dox
382 ($-33.4 \pm 7.9\%$ vs APP/PS1, $P = 0.02$ using Student's *t*-test; **Figure 5A**). In the cortex,
383 while Dox treatment did not change the levels of most markers, we observed a
384 significant decreased in NR2B protein levels as well as of its phosphorylation at Y1472
385 (NR2B: $-28.7 \pm 5.3\%$ vs. APP/PS1, $P = 0.02$; pY1472 NR2B: $-36.9 \pm 7.4\%$ vs APP/PS1,
386 $P = 0.02$ using Student's *t*-test; **Figure 5B**). These data suggest that Dox enhances the
387 level of several synaptic markers in the hippocampus while remains largely ineffective
388 in the cortex.

389

390 **DISCUSSION**

391

392 Doxycycline is a safe second-generation tetracycline which has been reported to exhibit
393 neuroprotective properties in various neurodegenerative models through, in particular,
394 its ability to slow down aggregation of misfolded proteins and to mitigate
395 neuroinflammatory processes (Santa-Cecília et al., 2019; Sultan et al., 2013). So far,
396 only one study tested Dox in a mouse model of amyloidogenesis which showed that
397 acute or subchronic Dox improved recognition memory and lower neuroinflammation
398 without altering plaques in APP/PS1 mice or animals injected i.c.v. with A β oligomers

399 (Balducci et al., 2018). In the present study, we reinvestigated Dox potential in
400 APP/PS1 mice and showed that Dox administered chronically and orally during 2
401 months provide a benefit, even moderate, to 9 month-old APP/PS1, particularly in the
402 long-term spatial memory. No major impact on the amyloid load has been observed.
403 However, memory improvement was associated with an enhancement of some synaptic
404 markers, in the hippocampus only. Puzzlingly, Dox also enhanced the mRNA
405 expression of various neuroinflammatory markers responsive to amyloid pathology.
406 Overall, the present data question the potential of Dox in the context of AD.
407 Our data, showing that oral Dox improves spatial memory abilities in APP/PS1 mice
408 (essentially in Barnes task), are in line the previous study of (Balducci et al., 2018)
409 which demonstrated that the acute or subchronic i.p. delivery of Dox mitigate A β -
410 induced memory deficits. This is in accordance with the improvement seen in
411 invertebrate A β models (Costa et al., 2011; De Luigi et al., 2008; Diomedede et al., 2010).
412 However, in sharp contrast with other studies (Forloni et al., 2001; Paldino et al., 2020)
413 which showed that Dox is prone to disassemble A β fibrils, the mouse studies of
414 (Balducci et al., 2018) were not able to observe an effect on amyloid plaques, even the
415 levels of A β oligomers in the hippocampus seemed reduced in APP/PS1 mice treated
416 with the antibiotic. However, we do not confirm the beneficial impact upon oligomers
417 and our data globally indicate that Dox does not impact amyloid load in APP/PS1 mice.
418 Surprisingly, spatial memory improvements of Dox-treated APP/PS1 animals was
419 associated with the enhancement of several hippocampal neuroinflammatory markers.
420 This is at odds with other reports supporting anti-inflammatory properties of Dox
421 (Balducci et al., 2018). Dox particulalry enhances CCL3, CCL4, Clec7a and Itgax that
422 are aged and AD associated genes, which suggest anyhow an immunomodulatory
423 impact of Dox (Benmamar-Badel et al., 2020). However, while CCL3 and CCL4 were

424 thought to significantly affects hippocampal plasticity and related memory (Carvalho et
425 al., 2021; Marciniak et al., 2015), although we cannot exclude that chemokines might
426 also exert beneficial effects on plasticity and memory as suggested by others (Ajoy et
427 al., 2021; Couturier et al., 2016; Kuijpers et al., 2010). It is therefore difficult to link
428 neuroinflammatory changes observed to spatial memory effects of Dox in APP/PS1.
429 Our data indicate that the antibiotic enhances the hippocampal level of several synaptic
430 proteins important for plasticity, notably GluR1, SNAP25 and Cofilin. The enhanced
431 level of the GluR1 subunit of AMPA receptors likely fits with memory improvement
432 (Mitsushima et al., 2011). Enhanced SNAP25 was likely associate with memory
433 improvement in models of AD (Ahmad et al., 2017; Tweedie et al., 2012). However, the
434 level of SNAP25 might also results in impaired memory (McKee et al., 2010) and, in
435 AD patients, higher SNAP25 has been associated with worse memory (Pereira et al.,
436 2021). The rise of Cofilin level remains also hard to firmly interpret. Indeed, actin
437 depolymerizing factor (ADF)/cofilin family of actin-associated proteins is important for
438 dendritic spine plasticity. (Gu et al., 2010) showed that cofilin-mediated actin dynamics
439 regulate AMPA receptor trafficking during synaptic potentiation, thereby improving
440 plasticity. In line, cofilin-1 conditional forebrain knock-out mice showed impaired late
441 phase LTP and LTD (Rust et al., 2010) and cofilin finely tunes synaptic function (Ben
442 Zablah et al., 2020). However, when levels of cofilin are elevated, they can also drive
443 the formation of cofilin-actin rods, as seen in the AD brain, which impairs synaptic
444 function. Then, genetic reduction of ADF/cofilin rescues neurodegeneration but also
445 LTP and contextual memory in APP/PS1 mice (Woo et al., 2015, 2012). Therefore, it
446 will be important to interpret these biochemical data in the light of future
447 electrophysiological recordings to clearly estimate the synaptic impact of Dox in
448 APP/PS1 mice and further argue on the therapeutical potential of this compound.

449 It is also noteworthy that Dox is largely used to regulate gene transcription in
450 conditional Tet-On and Tet-Off transgenic mouse models (Sprengel and Hasan, 2007).
451 Several Tet-On models of neurodegeneration are particularly used (Jankowsky and
452 Zheng, 2017; Khlistunova et al., 2006; Liu et al., 2015)((). Our data therefore highlight
453 that activating the expression of neuropathologically-relevant genes in the brain with
454 Dox might potentially interferes with the pathological processes by themselves and
455 those careful controls are warranted to address that issue.

456 While Dox has not been tested as a monotherapy in AD patients, two clinical trials
457 associating Dox with another antibiotic, rifampin, provided different outcomes. A first
458 trial suggested positive cognitive outcomes (Loeb et al., 2004) while the second failed
459 to reproduce a benefit (Molloy et al., 2013). While reasons for such discrepancies
460 remain unclear (dose, association therapy....), our findings are not overall arguing for a
461 clear potential of Dox in AD. In conclusion, while in a reliable model of AD, Dox is
462 prone to improve memory, the molecular and neuropathological changes induced by
463 this antibiotics need further investigation to define its real potential for further clinical
464 development in the AD context.

465

466 **FIGURE LEGENDS**

467

468 **Figure 1. Impact of chronic doxycycline on the spatial memory of APP/PS1 mice.**

469 (A-B) Actimetry. No impact of Dox on spontaneous locomotion was in both WT and
470 APP/PS1 mice. (C-D). Y-maze task. (C) During learning phase, mice spent a similar
471 percentage of time in the familiar arm vs the start arm. (D) In the test phase, the
472 discrimination index was found similar regardless genotype and treatment (Two-Way
473 ANOVA). However, all groups, except the APP mice, exhibited a percentage of time in

474 the novel arm significantly higher than the theoretical mean of 50% (dashed line). (E-F)
475 Barnes Maze. (E) Evaluation of the path length needed to find the hidden platform
476 during the spatial learning phase. During the 4 days of training, there was no significant
477 genotype x treatment x time difference (RM Two-Way analysis). (F) Spatial memory
478 was assessed 24h after the last training session. The percentage of time spent in the
479 target quadrant by APP mice was significantly lower as compared to WT mice
480 (* $p < 0.05$, Two-Way ANOVA followed by Tukey's multiple comparison test) while it
481 remained similar to WT for APP dox animals (NS). Moreover, the percentage of time
482 spent in the target quadrant was found significantly different from the theoretical mean
483 (ie. 25%, dashed line) for all groups but APP. Results are expressed as mean \pm s.e.m.
484 N=7-13 animals per group.

485

486 **Figure 2. Impact of Doxycycline on hippocampal and cortical amyloid pathology.**

487 (A) Hippocampal, cortical, and plasmatic levels of A β 1-40 and A β 1-42, assessed by
488 Elisa, showing no difference between APP/PS1 and APP/PS1 Dox groups. (B) A β
489 oligomers levels quantified by Elisa. Levels were increased in the cortex of Dox-treated
490 APP/PS1 mice vs. control APP/PS1 animals. ^{###} $P < 0.001$ vs APP/PS1 mice using
491 Student's t-test. (C) Representative pictures of 6E10-positive amyloid plaques in cortex
492 and hippocampus of APP/PS1 mice treated or not by Dox (Scale bars = 500 μ m). (D)
493 (a,c) Global A β load in the hippocampus and the cortex of APP and APP dox mice,
494 evaluated by the % of 6E10 surface stained. (b,d) Distribution of low vs large size
495 amyloid plaques in both structures. No effect of Dox could be observed (E-F) Western
496 blot evaluation of APP, C-terminal fragments (CTFs), total A β (6E10) and A β 1-42
497 (21F12) in the hippocampus (E) and cortex (F) of APP/PS1 mice treated or not by Dox.
498 No change could be observed except a slight increase of APP (APP C-17) in the cortex

499 in Dox-treated animals. [#]*P*<0.05 vs APP/PS1 mice using Student's t-test. Results are
500 expressed as mean ±s.e.m. N=7-9 animals per group.

501

502 **Figure 3. Impact of Doxycycline on hippocampal and cortical glial activation.**

503 Effect of doxycycline on glial activation was determined through Iba1 (microglia; **A**)
504 and GFAP (astrocytes; **B**) immunoreactivities. Graphs showed an increased level of
505 percentage of immunoreactive area for Iba1 and GFAP in APP/PS1 mice with no
506 impact of the Dox treatment. ** *P*<0.01, *** *P*<0.001 vs WT mice using Two-Way
507 ANOVA followed by Tukey's post hoc test. Scale bars = 200µm. Results are expressed
508 as mean ±s.e.m of the average quantification of 4-7 sections per animals with N=6-8
509 animals per group.

510

511 **Figure 4. Impact of Doxycycline on hippocampal and cortical neuroinflammation.**

512 Hippocampal and cortical neuro-inflammation was evaluated in all experimental groups
513 using quantitative PCR for markers of astrocytic activation (GFAP), microglial
514 activation (CD68 and C1qa), chemokines/cytokines (CCL3, CCL4 and TNFα), and
515 inflammatory receptors (TLR2, Clec7a, Itgax). All markers except TNFα were found
516 significantly upregulated in APP/PS1 mice as compared to WT animals (WT vs. APP
517 comparisons represented by *). In the hippocampus, rise of Clec7a, Itgax, CCL3 and
518 CCL4 in APP/PS1 mice was further enhanced by Dox (APP vs. APP Dox comparisons
519 represented by #). In the cortex, CCL4 was also increased by Dox treatment in APP/PS1
520 mice. **P*<0.05, ***P*<0.01, ****P*<0.001 vs WT mice, ##*P*<0.01 and ###*P*<0.001 vs
521 APP/PS1 mice using Two-Way ANOVA followed by Tukey's post hoc test. Results are
522 expressed as mean ±s.e.m. N=7-9 animals per group.

523

524 **Figure 5. Impact of Doxycycline on hippocampal and cortical synaptic markers.**

525 Western blot evaluation of NMDA receptor (NR1, NR2A, NR2B, p1472 NR2B),
526 AMPA receptors (GluR1, GluR2), pre-synaptic (Munc18, SNAP25) and post-synaptic
527 (PSD95, Cofilin) markers as well as NSE neuronal marker in the hippocampus of
528 APP/PS1 treated or not by Dox. In the hippocampus, GluR1, SNAP25, Cofilin were
529 found increased in APP/PS1 mice treated with Dox while Munc18 was rather
530 decreased). In the cortex, Dox treatment led to a decrease of NR2B and p-Y1472NR2B.
531 # $P < 0.05$ and ## $P < 0.01$ vs APP/PS1 mice using Student's t-test. Results are expressed
532 as mean \pm s.e.m. N=4-8 per group

533 **FUNDINGS**

534

535 This work was supported by grants from Programmes d'Investissements d'Avenir
536 LabEx (excellence laboratory) DISTALZ (Development of Innovative Strategies for a
537 Transdisciplinary approach to ALzheimer's disease). Our laboratories are also
538 supported by ANR (ADORASTrAU, METABOTAU, JANUS), COEN (5008),
539 Fondation pour la Recherche Médicale, France Alzheimer/Fondation de France,
540 Fondation Plan Alzheimer as well as Inserm, CNRS, Université Lille, Lille Métropole
541 Communauté Urbaine. VG-M was supported by Fondation pour la Recherche Médicale
542 (SPF20160936000).

543

544 **ACKNOWLEDGMENTS**

545

546 We thank the Plateformes Lilloises en Biologie et Santé (PLBS) - UMS 2014 - US 41:
547 Cell imaging, Animal Facilities, In vivo Imaging and function platform (F-59000 Lille,
548 France).

549 **AUTHOR CONTRIBUTIONS**

550

551 V.Gomez, K.Carvalho, B.Thiroux, R.Caillierez M.Besegher and E.Faivre performed
552 experiments, analyzed data, and corrected the manuscript. E. Faivre, N. Sergeant,
553 L.Buée, and D.Blum supervised the work, analyzed data, and wrote the manuscript.

554

555 **REFERENCES**

556

557 Ahmad, A., Ali, T., Park, H.Y., Badshah, H., Rehman, S.U., Kim, M.O., 2017.
558 Neuroprotective Effect of Fisetin Against Amyloid-Beta-Induced
559 Cognitive/Synaptic Dysfunction, Neuroinflammation, and Neurodegeneration in
560 Adult Mice. *Mol. Neurobiol.* 54, 2269–2285. [https://doi.org/10.1007/s12035-016-](https://doi.org/10.1007/s12035-016-9795-4)
561 9795-4

562 Ajoy, R., Lo, Y.C., Ho, M.H., Chen, Y.Y., Wang, Y., Chen, Y.H., Jing-Yuan, C.,
563 Changou, C.A., Hsiung, Y.C., Chen, H.M., Chang, T.H., Lee, C.Y., Chiang, Y.H.,
564 Chang, W.C., Hoffer, B., Chou, S.Y., 2021. CCL5 promotion of bioenergy
565 metabolism is crucial for hippocampal synapse complex and memory formation.
566 *Mol. Psychiatry.* <https://doi.org/10.1038/s41380-021-01103-3>

567 Balducci, C., Santamaria, G., La Vitola, P., Brandi, E., Grandi, F., Viscomi, A.R., Beeg,
568 M., Gobbi, M., Salmona, M., Ottonello, S., Forloni, G., 2018. Doxycycline
569 counteracts neuroinflammation restoring memory in Alzheimer’s disease mouse
570 models. *Neurobiol. Aging* 70, 128–139.
571 <https://doi.org/10.1016/j.neurobiolaging.2018.06.002>

572 Ben Zablah, Y., Merovitch, N., Jia, Z., 2020. The Role of ADF/Cofilin in Synaptic
573 Physiology and Alzheimer’s Disease. *Front. Cell Dev. Biol.* 8, 1–20.
574 <https://doi.org/10.3389/fcell.2020.594998>

575 Benmamar-Badel, A., Owens, T., Wlodarczyk, A., 2020. Protective Microglial Subset
576 in Development, Aging, and Disease: Lessons From Transcriptomic Studies. *Front.*
577 *Immunol.* 11. <https://doi.org/10.3389/fimmu.2020.00430>

578 Canas, P.M., Simões, A.P., Rodrigues, R.J., Cunha, R.A., 2014. Predominant loss of
579 glutamatergic terminal markers in a β -amyloid peptide model of Alzheimer’s

580 disease. *Neuropharmacology* 76, 51–56.
581 <https://doi.org/10.1016/j.neuropharm.2013.08.026>

582 Carvalho, K., Martin, E., Ces, A., Sarrazin, N., Lagouge-Roussey, P., Nous, C.,
583 Boucherit, L., Youssef, I., Prigent, A., Faivre, E., Eddarkaoui, S., Gauvrit, T.,
584 Vieau, D., Boluda, S., Huin, V., Fontaine, B., Buée, L., Delatour, B., Dutar, P.,
585 Sennlaub, F., Guillonneau, X., Blum, D., Delarasse, C., 2021. P2X7-deficiency
586 improves plasticity and cognitive abilities in a mouse model of Tauopathy. *Prog.*
587 *Neurobiol.* 206. <https://doi.org/10.1016/j.pneurobio.2021.102139>

588 Costa, R., Speretta, E., Crowther, D.C., Cardoso, I., 2011. Testing the therapeutic
589 potential of doxycycline in a *Drosophila melanogaster* model of Alzheimer disease.
590 *J. Biol. Chem.* 286, 41647–41655. <https://doi.org/10.1074/jbc.M111.274548>

591 Couturier, J., Stancu, I.C., Schakman, O., Pierrot, N., Huaux, F., Kienlen-Campard, P.,
592 Dewachter, I., Octave, J.N., 2016. Activation of phagocytic activity in astrocytes
593 by reduced expression of the inflammasome component ASC and its implication in
594 a mouse model of Alzheimer disease. *J. Neuroinflammation* 13, 1–13.
595 <https://doi.org/10.1186/s12974-016-0477-y>

596 D. Orsucci, V. Calsolaro, M. Mancuso, G.S., 2009. Neuroprotective Effects of
597 Tetracyclines: Molecular Targets, Animal Models and Human Disease.
598 <https://doi.org/10.2174/187152709788680689>

599 De Luigi, A., Colombo, L., Diomede, L., Capobianco, R., Mangieri, M., Miccolo, C.,
600 Limido, L., Forloni, G., Tagliavini, F., Salmona, M., 2008. The efficacy of
601 tetracyclines in peripheral and intracerebral prion infection. *PLoS One* 3.
602 <https://doi.org/10.1371/journal.pone.0001888>

603 Dennis J. Selkoe, 2002. Alzheimer's Disease Is a Synaptic Failure. *Science* (80-.). 298,
604 789–791.

605 Diomede, L., Cassata, G., Fiordaliso, F., Salio, M., Ami, D., Natalello, A., Doglia,
606 S.M., De Luigi, A., Salmona, M., 2010. Tetracycline and its analogues protect
607 *Caenorhabditis elegans* from β amyloid-induced toxicity by targeting oligomers.
608 *Neurobiol. Dis.* 40, 424–431. <https://doi.org/10.1016/j.nbd.2010.07.002>

609 Domercq, M., Matute, C., 2004. Neuroprotection by tetracyclines. *Trends Pharmacol.*
610 *Sci.* 25, 609–612. <https://doi.org/10.1016/j.tips.2004.10.001>

611 Faivre, E., Coelho, J.E., Zornbach, K., Malik, E., Baqi, Y., Schneider, M., Cellai, L.,
612 Carvalho, K., Sebda, S., Figeac, M., Eddarkaoui, S., Caillierez, R., Chern, Y.,
613 Heneka, M., Sergeant, N., Müller, C.E., Halle, A., Buée, L., Lopes, L. V., Blum,

614 D., 2018. Beneficial effect of a selective adenosine A2A receptor antagonist in the
615 APPswe/PS1dE9 mouse model of Alzheimer's disease. *Front. Mol. Neurosci.* 11,
616 1–13. <https://doi.org/10.3389/fnmol.2018.00235>

617 Forloni, G., Colombo, L., Girola, L., Tagliavini, F., Salmona, M., 2001. Anti-
618 amyloidogenic activity of tetracyclines: Studies in vitro. *FEBS Lett.* 487, 404–407.
619 [https://doi.org/10.1016/S0014-5793\(00\)02380-2](https://doi.org/10.1016/S0014-5793(00)02380-2)

620 Garcia-Alloza, M., Robbins, E.M., Zhang-Nunes, S.X., Purcell, S.M., Betensky, R.A.,
621 Raju, S., Prada, C., Greenberg, S.M., Bacsikai, B.J., Frosch, M.P., 2006.
622 Characterization of amyloid deposition in the APPswe/PS1dE9 mouse model of
623 Alzheimer disease. *Neurobiol. Dis.* 24, 516–524.
624 <https://doi.org/10.1016/j.nbd.2006.08.017>

625 Gu, J., Lee, C.W., Fan, Y., Komlos, D., Tang, X., Sun, C., Yu, K., Hartzell, H.C., Chen,
626 G., Bamberg, J.R., Zheng, J.Q., 2010. ADF/cofilin-mediated actin dynamics
627 regulate AMPA receptor trafficking during synaptic plasticity. *Nat. Neurosci.* 13,
628 1208–1215. <https://doi.org/10.1038/nn.2634>

629 Haïk, S., Marcon, G., Mallet, A., Tettamanti, M., Welaratne, A., Giaccone, G., Azimi,
630 S., Pietrini, V., Fabreguettes, J.R., Imperiale, D., Cesaro, P., Buffa, C., Aucan, C.,
631 Lucca, U., Peckeu, L., Suardi, S., Tranchant, C., Zerr, I., Houillier, C., Redaelli,
632 V., Vespignani, H., Campanella, A., Sellal, F., Krasnianski, A., Seilhean, D.,
633 Heinemann, U., Sedel, F., Canovi, M., Gobbi, M., Di Fede, G., Laplanche, J.L.,
634 Pocchiari, M., Salmona, M., Forloni, G., Brandel, J.P., Tagliavini, F., 2014.
635 Doxycycline in Creutzfeldt-Jakob disease: A phase 2, randomised, double-blind,
636 placebo-controlled trial. *Lancet Neurol.* 13, 150–158.
637 [https://doi.org/10.1016/S1474-4422\(13\)70307-7](https://doi.org/10.1016/S1474-4422(13)70307-7)

638 Heneka, M.T., Carson, M.J., Khoury, J. El, Gary, E., Brosseron, F., Feinstein, D.L.,
639 Jacobs, A.H., Wyss-coray, T., Vitorica, J., Ransohoff, R.M., 2018. HHS Public
640 Access Neuroinflammation in Alzheimer ' s Disease. *Lancet Neurol* 14, 388–405.
641 [https://doi.org/10.1016/S1474-4422\(15\)70016-5](https://doi.org/10.1016/S1474-4422(15)70016-5).Neuroinflammation

642 Jankowsky, J.L., Slunt, H.H., Ratovitski, T., Jenkins, N.A., Copeland, N.G., Borchelt,
643 D.R., 2001. Co-expression of multiple transgenes in mouse CNS: A comparison of
644 strategies. *Biomol. Eng.* 17, 157–165. [https://doi.org/10.1016/S1389-](https://doi.org/10.1016/S1389-0344(01)00067-3)
645 [0344\(01\)00067-3](https://doi.org/10.1016/S1389-0344(01)00067-3)

646 Jankowsky, J.L., Zheng, H., 2017. Practical considerations for choosing a mouse model
647 of Alzheimer's disease. *Mol. Neurodegener.* 12, 1–22.

648 <https://doi.org/10.1186/s13024-017-0231-7>

649 Khlistunova, I., Biernat, J., Wang, Y., Pickhardt, M., Von Bergen, M., Gazova, Z.,
650 Mandelkow, E., Mandelkow, E.M., 2006. Inducible expression of tau repeat
651 domain in cell models of tauopathy: Aggregation is toxic to cells but can be
652 reversed by inhibitor drugs. *J. Biol. Chem.* 281, 1205–1214.
653 <https://doi.org/10.1074/jbc.M507753200>

654 Kirvell, S.L., Esiri, M., Francis, P.T., 2006. Down-regulation of vesicular glutamate
655 transporters precedes cell loss and pathology in Alzheimer's disease. *J.*
656 *Neurochem.* 98, 939–950. <https://doi.org/10.1111/j.1471-4159.2006.03935.x>

657 Kuijpers, M., van Gassen, K.L.I., de Graan, P.N.E., Gruol, D., 2010. Chronic exposure
658 to the chemokine CCL3 enhances neuronal network activity in rat hippocampal
659 cultures. *J. Neuroimmunol.* 229, 73–80.
660 <https://doi.org/10.1016/j.jneuroim.2010.07.004>

661 Laurent, C., Buée, L., Blum, D., 2018. Tau and neuroinflammation: What impact for
662 Alzheimer's Disease and Tauopathies? *Biomed. J.* 41, 21–33.
663 <https://doi.org/10.1016/j.bj.2018.01.003>

664 Liu, P., Paulson, J.B., Forster, C.L., Shapiro, S.L., Ashe, K.H., Zahs, K.R., 2015.
665 Characterization of a novel mouse model of Alzheimer's disease - Amyloid
666 pathology and unique β -amyloid oligomer profile. *PLoS One* 10, 1–26.
667 <https://doi.org/10.1371/journal.pone.0126317>

668 Loeb, M.B., Molloy, D.W., Smieja, M., Standish, T., Goldsmith, C.H., Mahony, J.,
669 Smith, S., Borrie, M., Decoteau, E., Davidson, W., McDougall, A., Gnarpe, J.,
670 O'Donnell, M., Chernesky, M., 2004. A Randomized, Controlled Trial of
671 Doxycycline and Rifampin for Patients with Alzheimer's Disease. *J. Am. Geriatr.*
672 *Soc.* 52, 381–387. <https://doi.org/10.1111/j.1532-5415.2004.52109.x>

673 Marciniak, E., Faivre, E., Dutar, P., Alves Pires, C., Demeyer, D., Caillierez, R.,
674 Laloux, C., Buée, L., Blum, D., Humez, S., 2015. The Chemokine MIP-1 α /CCL3
675 impairs mouse hippocampal synaptic transmission, plasticity and memory. *Sci.*
676 *Rep.* 5, 1–11. <https://doi.org/10.1038/srep15862>

677 McKee, A.G., Loscher, J.S., O'Sullivan, N.C., Chadderton, N., Palfi, A., Batti, L.,
678 Sheridan, G.K., O'Shea, S., Moran, M., McCabe, O., Fernández, A.B., Pangalos,
679 M.N., O'Connor, J.J., Regan, C.M., O'Connor, W.T., Humphries, P., Farrar, G.J.,
680 Murphy, K.J., 2010. AAV-mediated chronic over-expression of SNAP-25 in adult
681 rat dorsal hippocampus impairs memory-associated synaptic plasticity. *J.*

682 Neurochem. 112, 991–1004. <https://doi.org/10.1111/j.1471-4159.2009.06516.x>

683 Mitsushima, D., Ishihara, K., Sano, A., Kessels, H.W., Takahashi, T., 2011. Contextual
684 learning requires synaptic AMPA receptor delivery in the hippocampus. *Proc. Natl.*
685 *Acad. Sci. U. S. A.* 108, 12503–12508. <https://doi.org/10.1073/pnas.1104558108>

686 Molloy, D.W., Standish, T.I., Zhou, Q., Guyatt, G., 2013. A multicenter, blinded,
687 randomized, factorial controlled trial of doxycycline and rifampin for treatment of
688 Alzheimer’s disease: The DARAD trial. *Int. J. Geriatr. Psychiatry* 28, 463–470.
689 <https://doi.org/10.1002/gps.3846>

690 Müller, U.C., Deller, T., Korte, M., 2017. Not just amyloid: Physiological functions of
691 the amyloid precursor protein family. *Nat. Rev. Neurosci.* 18, 281–298.
692 <https://doi.org/10.1038/nrn.2017.29>

693 Paldino, E., Balducci, C., La Vitola, P., Artioli, L., D’Angelo, V., Giampà, C., Artuso,
694 V., Forloni, G., Fusco, F.R., 2020. Neuroprotective Effects of Doxycycline in the
695 R6/2 Mouse Model of Huntington’s Disease. *Mol. Neurobiol.* 57, 1889–1903.
696 <https://doi.org/10.1007/s12035-019-01847-8>

697 Pereira, J.B., Janelidze, S., Ossenkoppele, R., Kvartsberg, H., Brinkmalm, A., Mattsson-
698 Carlgren, N., Stomrud, E., Smith, R., Zetterberg, H., Blennow, K., Hansson, O.,
699 2021. Untangling the association of amyloid- β and tau with synaptic and axonal
700 loss in Alzheimer’s disease. *Brain* 144, 310–324.
701 <https://doi.org/10.1093/brain/awaa395>

702 Rust, M.B., Gurniak, C.B., Renner, M., Vara, H., Morando, L., Görlich, A., Sassoè-
703 Pognetto, M., Banhaabouchi, M. Al, Giustetto, M., Triller, A., Choquet, D.,
704 Witke, W., 2010. Learning, AMPA receptor mobility and synaptic plasticity
705 depend on n-cofilin-mediated actin dynamics. *EMBO J.* 29, 1889–1902.
706 <https://doi.org/10.1038/emboj.2010.72>

707 Santa-Cecília, F.V., Leite, C.A., Del-Bel, E., Raisman-Vozari, R., 2019. The
708 Neuroprotective Effect of Doxycycline on Neurodegenerative Diseases. *Neurotox.*
709 *Res.* 35, 981–986. <https://doi.org/10.1007/s12640-019-00015-z>

710 Savonenko, A., Xu, G.M., Melnikova, T., Morton, J.L., Gonzales, V., Wong, M.P.F.,
711 Price, D.L., Tang, F., Markowska, A.L., Borchelt, D.R., 2005. Episodic-like
712 memory deficits in the APP^{swE}/PS1^{dE9} mouse model of Alzheimer’s disease:
713 Relationships to β -amyloid deposition and neurotransmitter abnormalities.
714 *Neurobiol. Dis.* 18, 602–617. <https://doi.org/10.1016/j.nbd.2004.10.022>

715 Sprengel, R., Hasan, M.T., 2007. Tetracycline-controlled genetic switches. *Handb. Exp.*

716 Pharmacol. 178, 49–72. https://doi.org/10.1007/978-3-540-35109-2_3

717 Sultan, S., Gebara, E., Toni, N., 2013. Doxycycline increases neurogenesis and reduces
718 microglia in the adult hippocampus. *Front. Neurosci.* 7, 1–10.
719 <https://doi.org/10.3389/fnins.2013.00131>

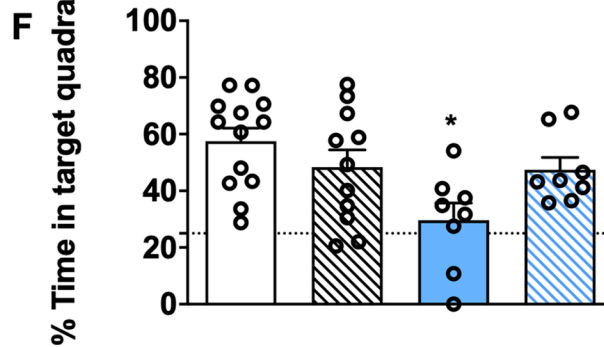
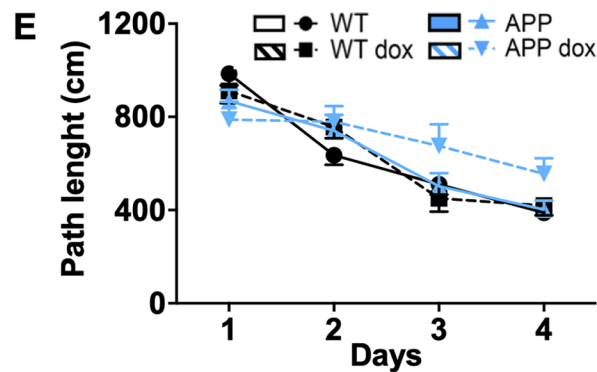
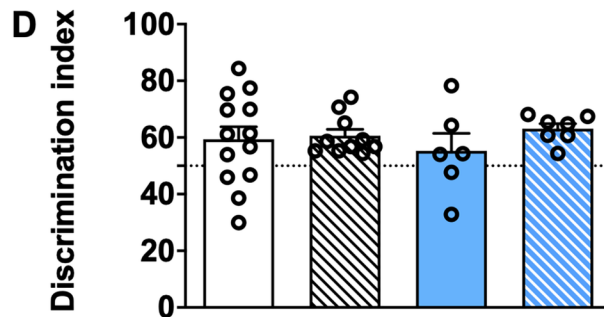
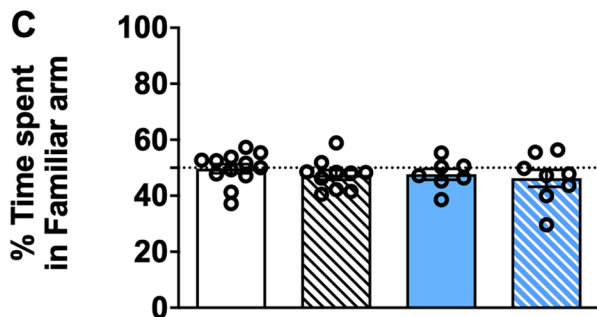
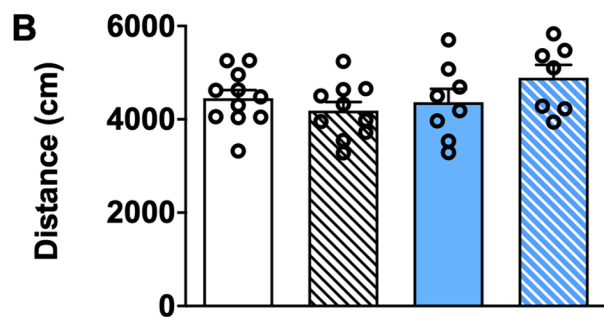
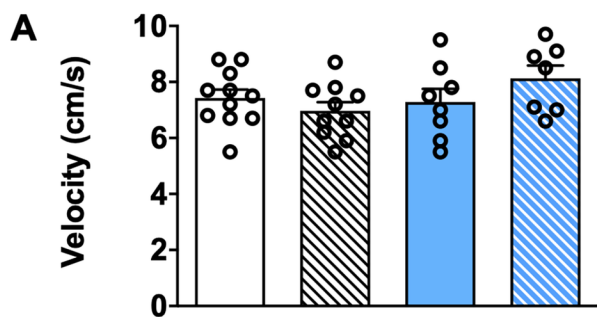
720 Tweedie, D., Ferguson, R.A., Fishman, K., Frankola, K.A., Van Praag, H., Holloway,
721 H.W., Luo, W., Li, Y., Caracciolo, L., Russo, I., Barlati, S., Ray, B., Lahiri, D.K.,
722 Bosetti, F., Greig, N.H., Rosi, S., 2012. Tumor necrosis factor- α synthesis inhibitor
723 3,6'-dithiothalidomide attenuates markers of inflammation, Alzheimer pathology
724 and behavioral deficits in animal models of neuroinflammation and Alzheimer's
725 disease. *J. Neuroinflammation* 9, 1. <https://doi.org/10.1186/1742-2094-9-106>

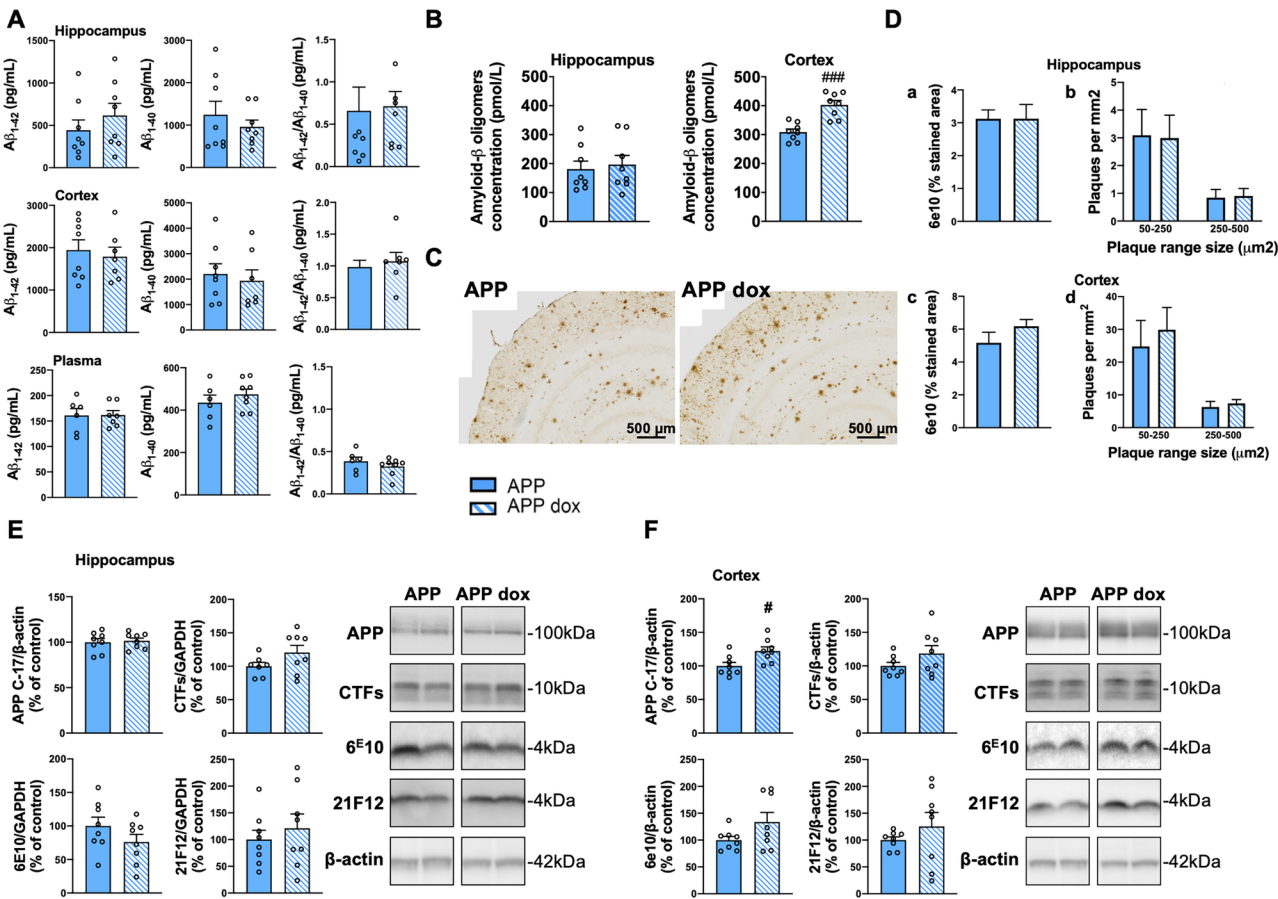
726 Woo, J.A., Boggess, T., Uhlar, C., Wang, X., Khan, H., Cappos, G., Joly-Amado, A.,
727 De Narvaez, E., Majid, S., Minamide, L.S., Bamburg, J.R., Morgan, D., Weeber,
728 E., Kang, D.E., 2015. RanBP9 at the intersection between cofilin and A β
729 pathologies: Rescue of neurodegenerative changes by RanBP9 reduction. *Cell*
730 *Death Dis.* 6, 1614–1676. <https://doi.org/10.1038/cddis.2015.37>

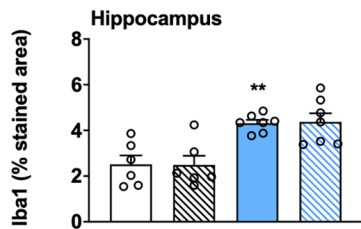
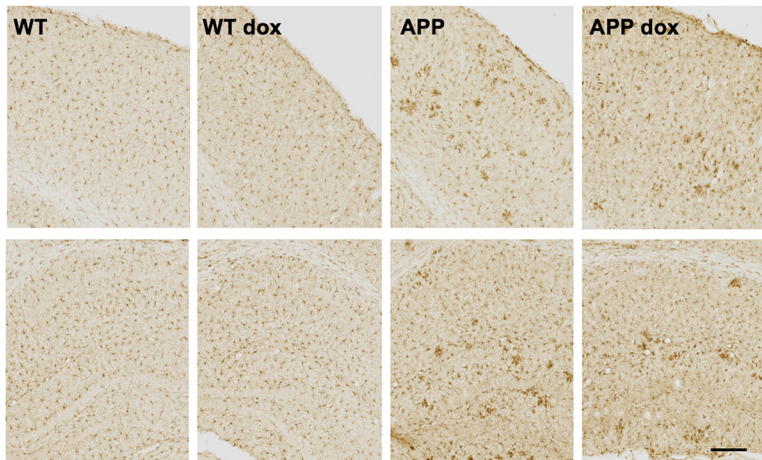
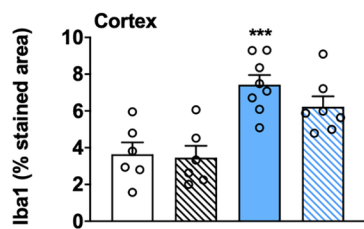
731 Woo, J.A., Jung, A.R., Lakshmana, M.K., Bedrossian, A., Lim, Y., Bu, J.H., Park, S.A.,
732 Koo, E.H., Mook-Jung, I., Kang, D.E., 2012. Pivotal role of the RanBP9-cofilin
733 pathway in AB-induced apoptosis and neurodegeneration. *Cell Death Differ.* 19,
734 1413–1423. <https://doi.org/10.1038/cdd.2012.14>

735 Zhang, W., Bai, M., Xi, Y., Hao, J., Liu, L., Mao, N., Su, C., Miao, J., Li, Z., 2012.
736 Early memory deficits precede plaque deposition in APP^{swe}/PS1^{dE9} mice:
737 Involvement of oxidative stress and cholinergic dysfunction. *Free Radic. Biol.*
738 *Med.* 52, 1443–1452. <https://doi.org/10.1016/j.freeradbiomed.2012.01.023>

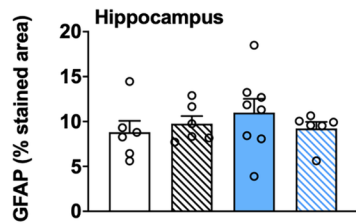
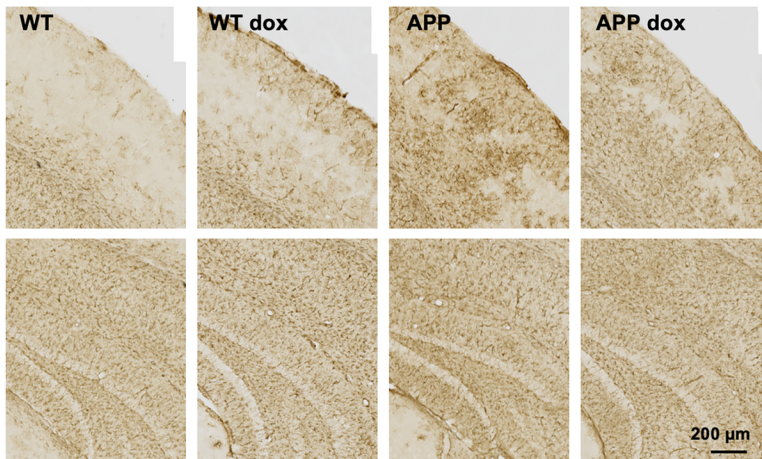
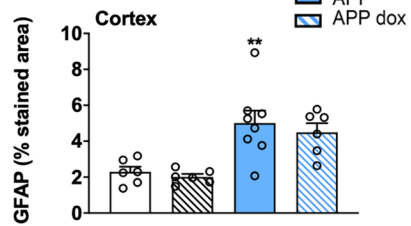
739 Zhou, Q., Wang, M., Du, Y., Zhang, W., Bai, M., Zhang, Z., Li, Z., Miao, J., 2015.
740 Inhibition of JNK activation reverses AD-Phenotypes in APP^{swe}/PS1^{dE9} Mice.
741 *Ann. Neurol.*



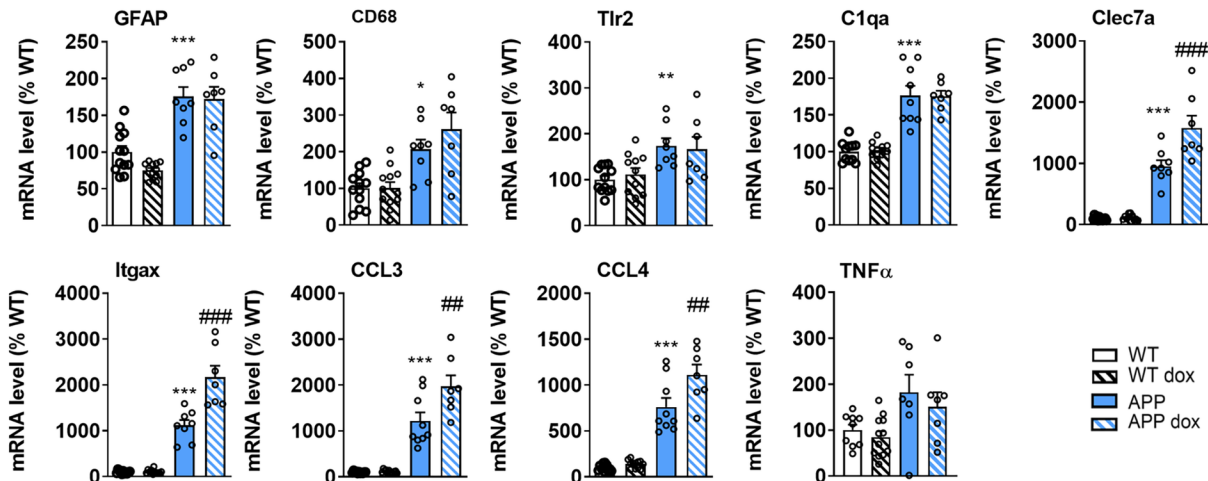
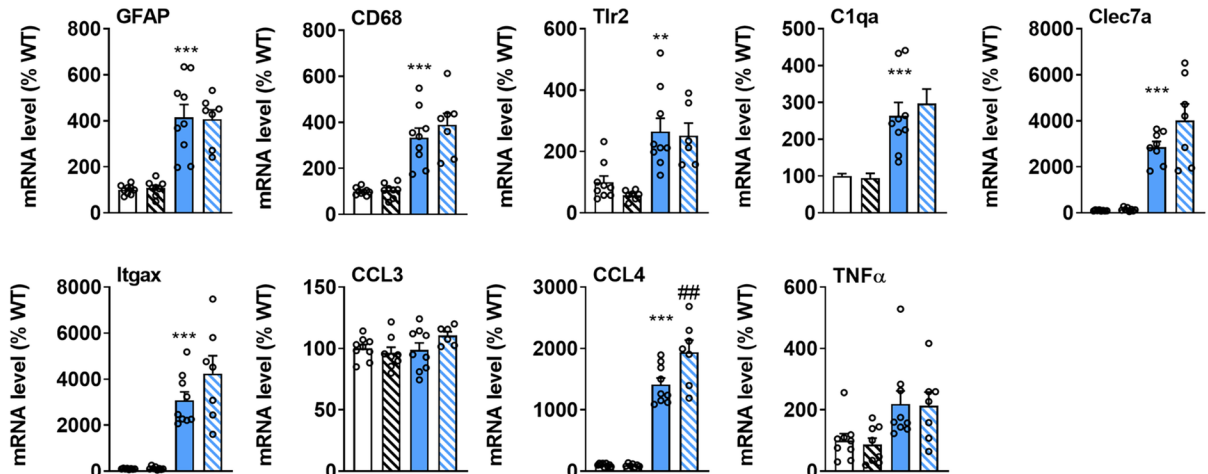


A

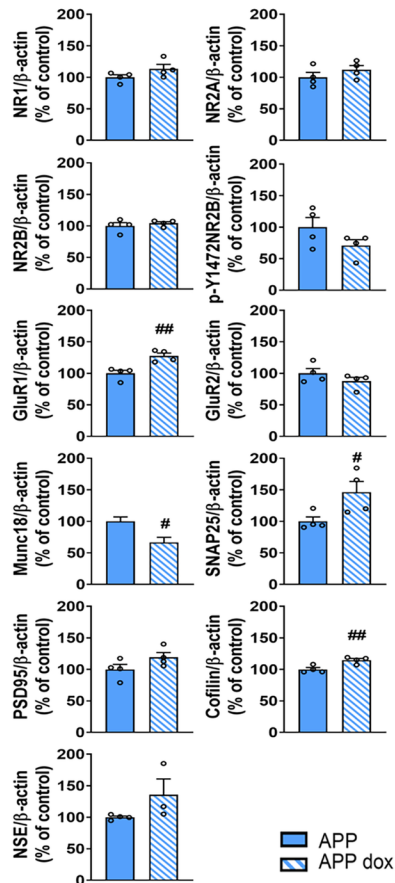
□ WT
 ▨ WT dox
 ■ APP
 ▩ APP dox

B

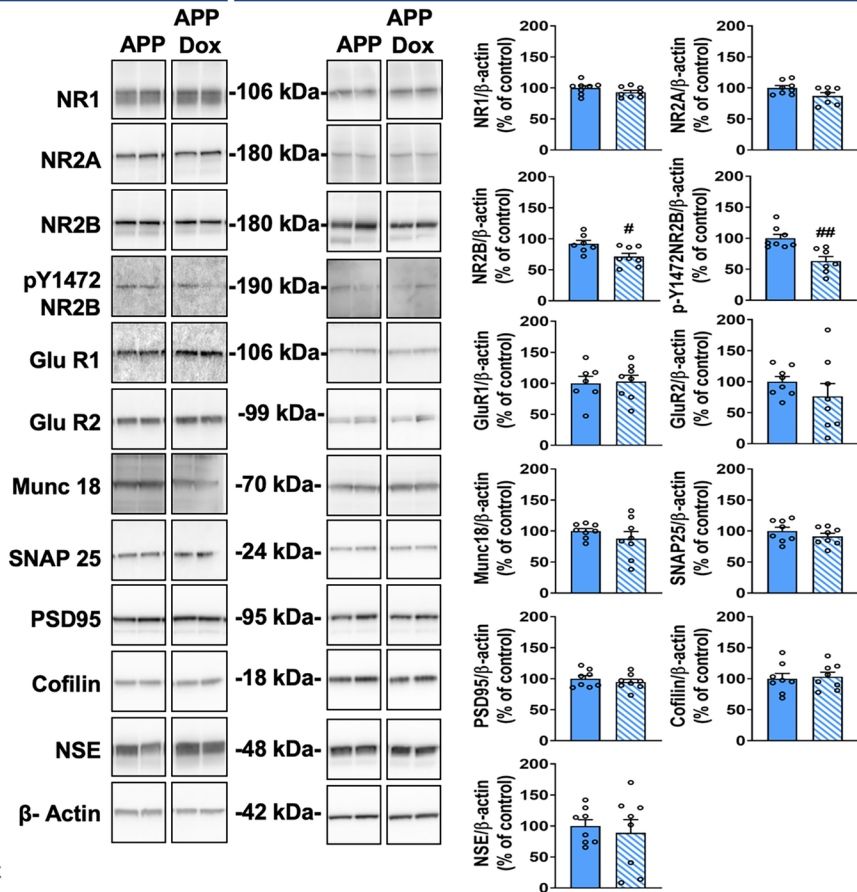
200 μ m

A**Hippocampus****B****Cortex**

A Hippocampus



B Cortex



Antibodies used				
Abbreviation	Origin	Provider	Reference	Dilution
β-actin	Rabbit	Sigma	A5441	1/10000
GAPDH	Mouse	Santa Cruz Biotechnology	25778	1/10000
NR2B	Rabbit	Millipore	06-600	1/1000
pY1472 NR2B	Rabbit	Cell Singaling	4208S	1/1000
NR2A	Rabbit	Cell Signaling	4205	1/1000
SNAP25	Mouse	Santa Cruz	376713	1/1000
Cofilin	Rabbit	abcam	ab134963	1/5000
NR1	Rabbit	Cell Signaling	5804	1/1000
Munc18	Rabbit	Sigma	M2694	1/2000
NSE	Rabbit	Life Science Enzo	BML-NA1247-0100	1/50000
GLUR1	Rabbit	Millipore	4855	1/5000
PSD95	Rabbit	Cell Singaling	2507S	1/1000
6e10	Mouse	Covance Biolegend	10LC0282	1/1000
21F12	Mouse	Homemade		1/2000
C-ter part of APP, CTFs	Rabbit	Homemade		1/5000
GluR2	Rabbit	Abcam	20673	1/5000
GFAP	Rabbit	Dako	Z03334	1/1000
Iba1	Rabbit	Wako	1919741	1/1000

MOUSE				
Primers	Accession number	Forward primer	Reverse primer	Amplicon length
Gfap	NM_001131020.1	CGCGAACAGGAAGAGCGCCA	GTGGCGGGCCATCTCCTCCT	104
Cd68	NM_009853.1	GACCTACATCAGAGCCCGAGT	CGCCATGAATGTCCACTG	95
Tlr2	NM_011905.3	GGGGCTTCACTTCTCTGCTT	AGCATCCTCTGCGATTGACG	110
Clec7a	NM_020008.2	ATGGTTCTGGGAGGATGGAT	GCTTTCCTGGGGAGCTGTAT	72
Itgax	NM_021334.2	ATGGAGCCTCAAGACAGGAC	GGATCTGGGATGCTGAAATC	62
Ccl3	NM_011337.2	TGCCCTTGCTGTTCTTCTCT	GTGGAATCTCCGGCTGTAG	112
Ccl4	NM_013652.2	GCCCTCTCTCCTCTTGCT	GAGGGTCAGAGCCCATG	72
Tnfa	NM_013693.2	TGCCTATGTCTCAGCCTTTC	GAGGCCATTTGGGAACTTCT	116
Cyclophilin A	NM_008907.1	AGCATACAGGTCTGGCATC	TTCACCTCCCAAAGACCAC	126
Taqman probe	Accession number	Assay ID	Assay Design	Amplicon length
C1qa	NM_007572.2	Mm00432142_m1	Probe spans exons	80
Cyclophilin A	NM_008907.1	Mm02342430_g1	Probe spans exons	148